



# Effect of illumination intensity on cell parameters of a silicon solar cell

Firoz Khan<sup>a,\*</sup>, S.N. Singh<sup>a</sup>, M. Husain<sup>b</sup>

<sup>a</sup> Electronic Materials Division, National Physical Laboratory (Council of Scientific and Industrial Research), Dr. K.S. Krishnan Marg, New Delhi-110012, India

<sup>b</sup> Department of Physics, Jamia Millia Islamia, New Delhi-110025, India

## ARTICLE INFO

### Article history:

Received 12 June 2009

Received in revised form

23 February 2010

Accepted 12 March 2010

Available online 2 April 2010

### Keywords:

Silicon solar cells

Cell parameters

Shunt resistance

Series resistance

Diode ideality factor

## ABSTRACT

The effect of illumination intensity  $P_{in}$  on the cell parameters of a silicon solar cell has been investigated based on one diode model. The variation of slopes of the  $I$ – $V$  curves of a cell at short circuit and open circuit conditions with intensity of illumination in small span of intensity has been applied to determine the cell parameters, viz. shunt resistance  $R_{sh}$ , series resistance  $R_s$ , diode ideality factor  $n$  and reverse saturation current  $I_0$  of the cell. The dependence of cell parameters on intensity has been investigated for a fairly wide illumination intensity range 15–180 mW/cm<sup>2</sup> of AM1.5 solar radiations by dividing this intensity range into a desirable number of small intensity ranges for measurements of the slopes of the  $I$ – $V$  curves at short circuit and open circuit conditions. Initially  $R_{sh}$  increases slightly with  $P_{in}$  and then becomes constant at higher  $P_{in}$  values. However,  $R_s$ ,  $n$  and  $I_0$  all decrease continuously with  $P_{in}$ , but the rate of decrease of each of these becomes smaller at higher  $P_{in}$  values. Theoretical values of open circuit voltage  $V_{oc}$ , curve factor CF and efficiency  $\eta$  calculated using the cell parameters determined by the present method match well with the corresponding experimental values.

© 2010 Elsevier B.V. All rights reserved.

## 1. Introduction

The steady state  $I$ – $V$  characteristics of a  $p$ – $n$  junction silicon solar cell are often described based on one diode model [1–3] as

$$I = -I_{ph} + I_0 \left( e^{\frac{q(V - IR_s)}{nkT}} - 1 \right) + \frac{(V - IR_s)}{R_{sh}} \quad (1)$$

In Eq. (1)  $I_{ph}$  is the light generated current,  $q$  is electron charge,  $k$  is Boltzmann constant and  $T$  is the temperature,  $R_{sh}$  is the shunt resistance,  $R_s$  is the series resistance,  $n$  is the diode ideality factor and  $I_0$  is the reverse saturation current of the cell.  $R_{sh}$ ,  $R_s$ ,  $n$ ,  $I_0$  are cell parameters of the cell. These cell parameters control the  $I$ – $V$  characteristics of a cell at any given intensity of illumination and cell temperature and thus decide the values of the performance parameters, viz. the short circuit current ( $I_{sc}$ ), open circuit voltage ( $V_{oc}$ ), curve factor (CF) and thereby the efficiency ( $\eta$ ) of the cell. As the intensity of illumination changes the values of performance parameters change significantly [4–7]. The dependence of performance parameters on illumination intensity can get affected if the values of the cell parameters  $R_{sh}$ ,  $R_s$ ,  $n$  and  $I_0$  themselves change with illumination intensity.

Therefore, it is important to evaluate all cell parameters  $R_{sh}$ ,  $R_s$ ,  $n$  and  $I_0$  and study their variation with illumination intensity. Variation of the cell parameters, viz.  $R_{sh}$  and  $R_s$  with illumination intensity has been investigated analytically by several researchers

[2,4,5]. However, the studies on the effect of illumination intensity on  $n$  and  $I_0$  are rather scarce in literature [8]. Datta et al. [8] have applied a computer aided curve fitting technique to determine the values of  $R_{sh}$ ,  $R_s$ ,  $n$  and  $I_0$  using  $I$ ,  $V$  values corresponding to the various points on a single  $I$ – $V$  curve obtained at a given intensity. They have determined the values of these parameters only at three values of  $P_{in}$  and their results do not show any clear trend of variation of these parameters with  $P_{in}$ .

Most silicon solar cells are designed to work under normal sunlight and their performances are evaluated at 25 °C under an AM1.5 solar irradiation of 100 mW/cm<sup>2</sup> intensity. Also, as stated earlier, the one diode model is most commonly used to describe the  $I$ – $V$  characteristics of a cell. Therefore, in this work, we have investigated the variation of cell parameters based on one diode model, viz.  $R_{sh}$ ,  $R_s$ ,  $n$  and  $I_0$  in the illumination intensity range 15–180 mW/cm<sup>2</sup>. For this purpose, we divide such a wide intensity range into a large number of smaller intensity ranges, wherein the cell parameters will remain constant. We determine values of all the four cell parameters of a silicon solar cell, analytically from the variation of slopes of the  $I$ – $V$  curve at short circuit and open circuit with  $P_{in}$  in all the smaller intensity ranges one after the other.

## 2. Theoretical

Denoting the slope  $dI/dV$  of  $I$ – $V$  curve at short circuit ( $V=0$ ,  $I = -I_{sc}$ ) by  $m_{sc}$  and that at open circuit ( $V=V_{oc}$ ,  $I=0$ ) by  $m_{oc}$  we

\* Corresponding author. Tel.: +91 11 45608330; fax: +91 11 45609310.  
E-mail address: [firozkphysics@gmail.com](mailto:firozkphysics@gmail.com) (F. Khan).

can obtain from Eq. (1) relations of slopes  $m_{sc}$  and  $m_{oc}$  with the cell parameters as

$$m_{sc} = \frac{\left[1/R_{sh} + qI_0/nkT e^{\frac{qI_{sc}R_s}{nkT}}\right]}{\left[1 + R_s \left\{1/R_{sh} + qI_0/nkT e^{\frac{qI_{sc}R_s}{nkT}}\right\}\right]} \quad (2)$$

$$m_{oc} = \frac{\left[1/R_{sh} + qI_0/nkT e^{\frac{qV_{oc}}{nkT}}\right]}{\left[1 + R_s \left\{1/R_{sh} + qI_0/nkT e^{\frac{qV_{oc}}{nkT}}\right\}\right]} \quad (3)$$

Eq. (2) shows that  $m_{sc}$  is related with the diode parameters ( $R_{sh}$ ,  $R_s$ ,  $n$  and  $I_0$ ) and  $I_{sc}$  of the cell. Similarly Eq. (3) shows that  $m_{oc}$  is related with the cell parameters and  $V_{oc}$  of the cell. Since both  $I_{sc}$  and  $V_{oc}$  depend on the intensity of illumination  $P_{in}$  we can expect both  $m_{sc}$  and  $m_{oc}$  to change with  $P_{in}$ , whether or not the cell parameters change with  $P_{in}$ .

Since a practical solar cell is designed to keep  $R_s$  small and  $R_{sh}$  large, the two conditions

$$\frac{qI_0}{nkT} e^{\frac{qI_{sc}R_s}{nkT}} \ll \frac{1}{R_{sh}} \quad (4)$$

and

$$\frac{qI_0}{nkT} e^{\frac{qV_{oc}}{nkT}} \gg \frac{1}{R_{sh}} \quad (5)$$

are satisfied simultaneously for a significantly wide  $P_{in}$  range of operation of the cell. We shall henceforth refer to it as a suitable  $P_{in}$  range. In this  $P_{in}$  range Eqs. (3) and (4) are simplified to give

$$m_{sc}^{-1} = (R_{sh} + R_s) \quad (6)$$

and

$$m_{oc}^{-1} = \left[ R_s + \frac{nkT}{qI_0} e^{-\left(\frac{qV_{oc}}{nkT}\right)} \right] \quad (7)$$

In this  $P_{in}$  range  $V_{oc} \gg I_{sc} R_s$ , hence,

$$I_0 e^{\frac{qV_{oc}}{nkT}} \approx I_{sc} = \frac{V_{oc}}{R_{sh}} \quad (8)$$

Substituting Eq. (8) into Eq. (7) we obtain

$$m_{oc}^{-1} = \left[ R_s + \frac{nkT}{q} \frac{1}{\left(I_{sc} - \frac{V_{oc}}{R_{sh}}\right)} \right] \quad (9)$$

Also because  $R_s \ll R_{sh}$ , Eq. (6) can be approximated as

$$R_{sh} = m_{sc}^{-1} \quad (10)$$

The combination of Eqs. (7), (9) and (10) can be used to determine representative values of  $R_{sh}$ ,  $R_s$ ,  $n$  and  $I_0$  of a cell from measurements of  $I_{sc}$ ,  $V_{oc}$ ,  $m_{sc}$  and  $m_{oc}$  at different intensities in a suitable range of  $P_{in}$ .

### 3. Experimental

The measurements for the present work were made on monocrystalline silicon (c-Si) solar cells of  $\sim 8 \text{ cm}^2$  area which were fabricated using 300  $\mu\text{m}$  thick,  $\langle 100 \rangle$  oriented p-Cz silicon wafer of  $1 \Omega \text{ cm}$  base resistivity. The p-n junction was made by P-diffusion using a  $\text{POCl}_3$  liquid source. Front and back contacts were realized by screen printing Ag paste on front and Ag/Al paste on back sides of the cells. A single layer silicon nitride anti-reflection coating was given by a PECVD process using  $\text{SiH}_4$ ,  $\text{NH}_3$  and  $\text{N}_2$  gases. Illuminated I-V characteristics of the cells were measured at  $25^\circ\text{C}$  at different intensities in small spans of intensity which together covered a fairly wide intensity range 15–180  $\text{mW/cm}^2$  of simulated AM 1.5 solar radiation. The cell with its n+ front emitter on top was mounted on a gold plated base which was maintained at a constant temperature using a

refrigerated water circulator Julabo Model F10. The cells were illuminated with a simulated AM1.5 global radiation and illuminated I-V characteristics were measured with the help of a KEITHLEY 2420 system sourceter. The illumination intensity was measured using a reference silicon solar cell obtained from PV Measurements, USA. In the following the results of measurements of cell parameters will be reported for a silicon solar cell, cell #1 fabricated as described above.

### 4. Result and discussion

A number of I-V curves were obtained for cell #1 in five small spans of intensity ranges, viz.  $15 < P_{in} < 31 \text{ mW/cm}^2$ ,  $35 < P_{in} < 55 \text{ mW/cm}^2$ ,  $60 < P_{in} < 80 \text{ mW/cm}^2$ ,  $95 < P_{in} < 122 \text{ mW/cm}^2$  and  $145 < P_{in} < 180 \text{ mW/cm}^2$ . The values of  $I_{sc}$ ,  $V_{oc}$ ,  $m_{sc}$  and  $m_{oc}$  of the I-V curves in each of the above  $P_{in}$  ranges were used to determine the cell parameters. The value of  $m_{sc}$  was nearly invariant with intensity and thereby yielded a constant value of  $R_{sh}$  according to Eq. (10). These values of  $R_{sh}$  were in turn used with  $I_{sc}$ ,  $V_{oc}$  and  $m_{oc}$  values to determine values of  $R_s$ ,  $n$  and  $I_0$  of the cell as described in the following for one intensity range, viz.  $15 < P_{in} < 31 \text{ mW/cm}^2$ .

The values of  $m_{oc}^{-1}$  were plotted against  $(I_{sc} - V_{oc}/R_{sh})^{-1}$  in  $15 < P_{in} < 31 \text{ mW/cm}^2$  range as shown in Fig. 1 and were fitted into a straight line represented by Eq. (9). The intercept of the straight line on  $m_{oc}^{-1}$  axis gave the value of  $R_s$  and the slope of the line with the  $(I_{sc} - V_{oc}/R_{sh})^{-1}$  axis yielded the value of  $nkT/q$ . The value of  $nkT/q$  thus obtained was used in Eq. (7) and, then, the plot of  $m_{oc}^{-1}$  vs.  $e^{-qV_{oc}/nkT}$  data and their subsequent fit into a straight line as shown in Fig. 2 yielded the value of  $I_0$  from its slope  $nkT/qI_0$  with the  $e^{-qV_{oc}/nkT}$  axis. The intercept of  $m_{oc}^{-1}$  vs.  $e^{-qV_{oc}/nkT}$  line on  $m_{oc}^{-1}$  axis of Fig. 2 also gave a value of  $R_s$ . Thus, the values of  $R_{sh}$ ,  $R_s$ ,  $n$  and  $I_0$  for cell #1 were determined for  $15 < P_{in} < 31 \text{ mW/cm}^2$  range. Similarly, the values  $R_{sh}$ ,  $R_s$ ,  $n$  and  $I_0$  for cell #1 for the remaining four small  $P_{in}$  ranges ( $35 < P_{in} < 55 \text{ mW/cm}^2$ ,  $60 < P_{in} < 80 \text{ mW/cm}^2$ ,  $95 < P_{in} < 122 \text{ mW/cm}^2$  and  $145 < P_{in} < 180 \text{ mW/cm}^2$ ) were also determined. The values of the cell parameters show that the conditions (4), (5) and Eqs. (8) and (9) have been fully valid for cell #1 in all the  $P_{in}$  ranges used in the measurements. The errors are less than 0.01%. The values of  $R_{sh}$ ,  $R_s$ ,  $n$  and  $I_0$  determined as above for different  $P_{in}$  ranges were assigned to the mean  $P_{in}$  value of the each  $P_{in}$  range.

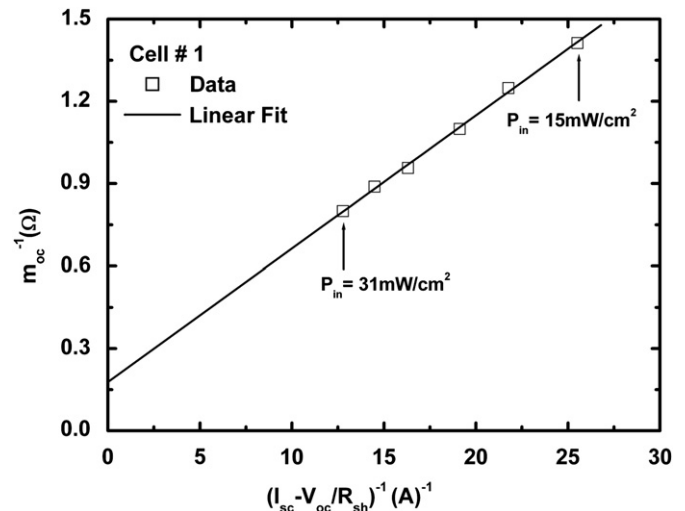


Fig. 1. Plot of  $m_{oc}^{-1}$  vs.  $(I_{sc} - V_{oc}/R_{sh})^{-1}$  curve for cell #1 at  $T=25^\circ\text{C}$  and small intensity range  $15 < P_{in} < 31 \text{ mW/cm}^2$ . The solid line gives a straight line fit to the data. The intercept on  $m_{oc}^{-1}$  axis gives  $R_s$ .

The cell parameters have been plotted against  $P_{in}$  in Fig. 3. It shows that  $R_{sh}$  increases slightly with  $P_{in}$  at lower  $P_{in}$  values and, then, becomes constant at higher intensities of illumination. Priyanka et al. [2] have also observed a similar dependence of  $R_{sh}$  on  $P_{in}$ . An increase in  $R_{sh}$  with  $P_{in}$  in the low intensity range (e.g.  $P_{in} < 50 \text{ mW/cm}^2$ ) has been observed also by Cunningham et al. [9] in PV modules based on single- and multi-crystalline silicon solar cells.

The increase of  $R_{sh}$  with  $P_{in}$  at low  $P_{in}$  values may be due to the existence of local inhomogeneities leading to non uniform current flow [10] or to charge leakage across the  $p$ – $n$  junction in the cell [11]. This is because generally shunt is associated with the localized defect regions which in turn have a larger concentration of traps that make them electrically active [11]. These traps act as sinks for majority carriers or photogenerated minority carriers depending on the nature of the traps [12,13]. The traps can be detected using Deep Level Transient Spectroscopy [12,14]. Traps capture carriers from the neighboring regions [13]. The electrical activity of traps is stronger at low current densities under dark or at low illumination intensities. In a solar cell, a defect region

makes a poor cell than the defect free region and both the cells are connected in parallel [10]. At any operational point above the short circuit, this gives rise to a circulation current. This is equivalent to a shunt current. As the illumination intensity increases the traps start getting filled and this reduces the shunt current and thus increases the shunt resistance of the cell. At a certain value of the illumination intensity, all traps get filled and then the shunt resistance attains a maximum value for further increase in the illumination intensity unless the high  $P_{in}$  causes some other effect, e.g. the heating of the cell, that may degrade the shunt resistance [15].

Fig. 3 also shows that  $R_s$  decreases continuously with increasing the intensity of illumination. However, the rate of decrease of  $R_s$  with  $P_{in}$  is much small for  $P_{in} > 70 \text{ mW/cm}^2$ . Earlier researchers [2,4,5,16] have also found  $R_s$  decreasing with  $P_{in}$ . As pointed out by Arora et al. [16], the decrease can be attributed it to the increase in conductivity of the active layer with the increase in the intensity of illumination.

Fig. 3 also depicts the dependence of  $n$  and  $I_0$  with  $P_{in}$ . The values of  $n > 1.5$  for  $P_{in} < 40 \text{ mW/cm}^2$  and decreases slowly with  $P_{in}$  from 1.5 at  $P_{in}=40 \text{ mW/cm}^2$  to 1.35 at  $P_{in}=160 \text{ mW/cm}^2$ . McDonald and Cuevas [17] have found  $n$  decreasing with  $V_{oc}$  monotonically in multicrystalline silicon solar cells made from  $1.5 \Omega\text{-cm}$  resistivity material which implied decrease of  $n$  with  $P_{in}$ . The value of  $I_0$  is  $5.5 \times 10^{-7} \text{ A}$  at  $P_{in}=20 \text{ mW/cm}^2$  and decreases at higher  $P_{in}$  values. In bifacial silicon solar cells, Ohtsuka et al. [18] have observed that  $I_0$  decreases with the increase in  $P_{in}$  under front, rear and bifacial illumination conditions.

In a silicon solar cell, the values of  $n$  and  $I_0$  are governed by the combination of space charge recombination, bulk recombination and surface recombination mechanisms. The space charge recombination is more effective at low intensities and low junction voltages. So the higher  $n$  and  $I_0$  values at lower intensities as shown in Fig. 3 can be attributed to the larger contribution of space charge recombination to the total recombination in the cell. The contribution of space recombination decreases at higher  $P_{in}$  and, then, the values of  $n$  and  $I_0$  owe their values increasingly to the bulk and surface recombination mechanisms.

The values of the cell parameters shown in Fig. 3 were used in Eq. (1) along with  $I_{sc}$  values to generate theoretical  $I$ – $V$  characteristics and calculate  $V_{oc}$ , CF and  $\eta$  values of cell #1 in  $15 < P_{in} < 180 \text{ mW/cm}^2$  intensity range. For cell #1,  $I_{sc}=I_{ph}$  has been valid in  $15 < P_{in} < 180 \text{ mW/cm}^2$  range. Theoretical values of

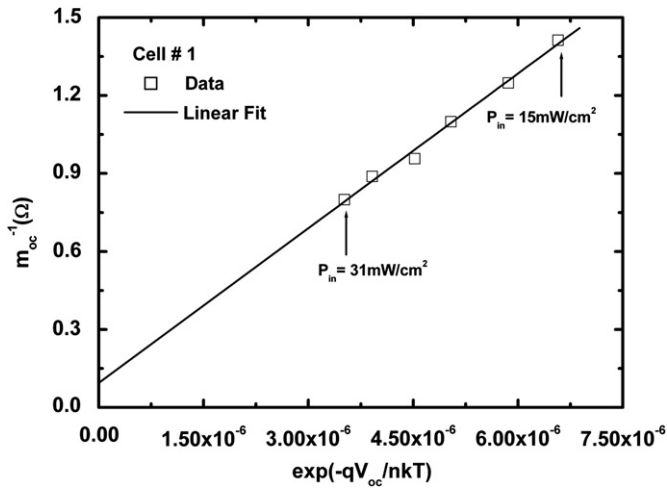


Fig. 2. Plot of  $m_{oc}^{-1}$  vs.  $e^{-qV_{oc}/nkT}$  curve for cell #1 at  $T=25^\circ\text{C}$  and  $15 < P_{in} < 31 \text{ mW/cm}^2$  with  $n=1.84$ ;  $n$  was obtained from Fig. 1. The solid line gives a straight line fit to the data. The slope of straight line with the  $e^{-qV_{oc}/nkT}$  axis determines  $I_0$  value.

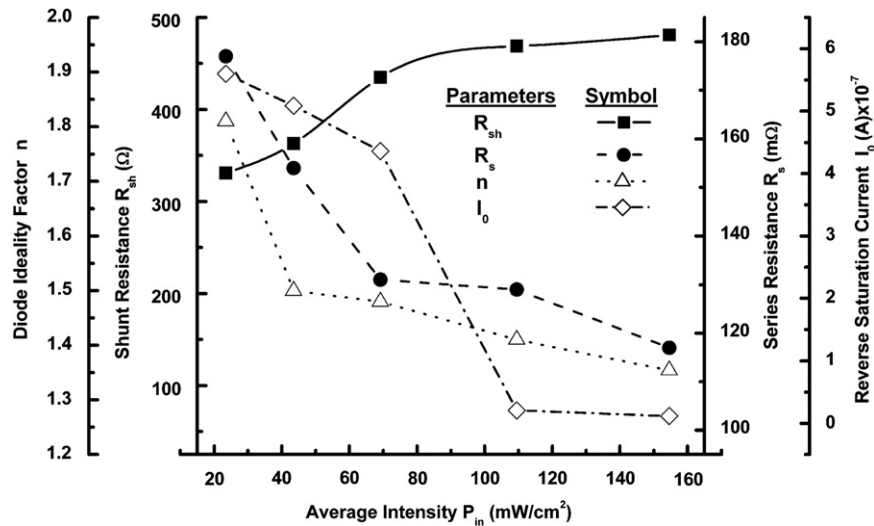
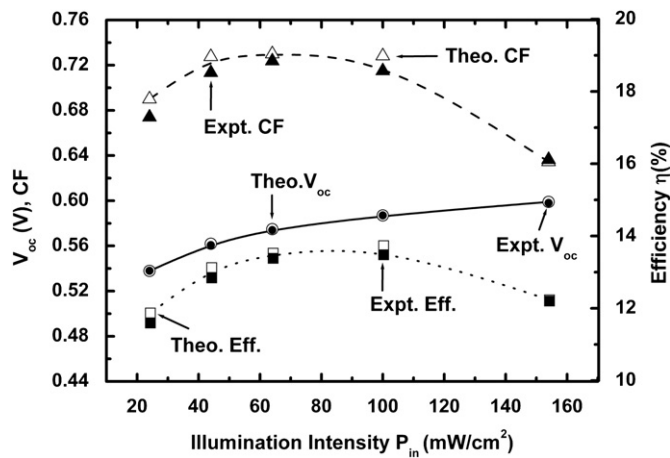


Fig. 3. Plot of the observed dependence of cell parameters viz.  $R_{sh}$  (—■—),  $R_s$  (---●---),  $n$  (····△····) and  $I_0$  (—◇—) on intensity of illumination for cell #1 at  $T=25^\circ\text{C}$  in  $15 < P_{in} < 180 \text{ mW/cm}^2$  intensity range of illumination. The left- and right-end data points correspond to  $P_{in}=24 \text{ mW/cm}^2$  and  $P_{in}=154 \text{ mW/cm}^2$ , respectively.



**Fig. 4.** Plots of the theoretical values of  $V_{oc}$  (—○—), CF (—□—) and  $\eta$  (—△—) obtained using the calculated values of the cell parameters with the experimental values  $V_{oc}$  (●), CF (■) and  $\eta$  (▲) at  $T=25^\circ\text{C}$  against intensity of illumination for  $15 < P_{in} < 180 \text{ mW/cm}^2$  range. The left- and right-end data points correspond to  $P_{in}=24 \text{ mW/cm}^2$  and  $P_{in}=154 \text{ mW/cm}^2$ , respectively.

$V_{oc}$ , CF and  $\eta$  are compared with the experimental values in Fig. 4. It can be noted that theoretical values of  $V_{oc}$ , CF and  $\eta$  match well with their experimental values obtained for  $24 < P_{in} < 154 \text{ mW/cm}^2$  range.

## 5. Conclusion

We have determined the values of cell parameters  $R_{sh}$ ,  $R_s$ ,  $n$  and  $I_0$  using the variation of  $m_{sc}$ ,  $m_{oc}$  with intensity in small  $P_{in}$  ranges and have applied this method to determine the dependence of the cell parameters with  $P_{in}$  in a fairly wide intensity range ( $15 < P_{in} < 180 \text{ mW/cm}^2$  range) by dividing it into a significantly large number of small intensity ranges. It is noted that initially  $R_{sh}$  increases with  $P_{in}$  and then become nearly constant. However,  $R_s$ ,  $n$  and  $I_0$  all decrease continuously with  $P_{in}$ . The rate of decrease of each of these parameters is higher at lower  $P_{in}$  values than at higher  $P_{in}$  values. Theoretical values of  $V_{oc}$ , CF and  $\eta$  obtained using the cell parameters determined by the present method match well with their corresponding experimental values. It shows that the present method of determination of the cell parameters from the slopes of  $I$ - $V$  curve at short circuit and open circuit conditions is applicable to determine the variation of the cell parameters with  $P_{in}$  over wide  $P_{in}$  range by dividing the  $P_{in}$  range into a desirable number of small intensity ranges.

## Acknowledgment

The authors are thankful to Director, National Physical Laboratory, New Delhi, for his permission to publish this paper. The author Firoz Khan gratefully acknowledges the support of Council of Scientific and Industrial Research (CSIR), India.

## References

- [1] S.K. Agarwal, R. Muralidharan, Amit Agarwal, V.K. Tiwary, S.C. Jain, A new method for the measurement of series resistance of solar cells, *Journal of Physics D: Applied Physics* 14 (1981) 1643–1646.
- [2] Mohan Lal Priyanka, S.N. Singh, A new method for the measurement of series and shunt resistance of silicon solar cells, *Solar Energy Materials and Solar Cells* 91 (2007) 137–142.
- [3] K. Raj Karan, J. Shewchun, A better approach to the evaluation of the series resistance of solar cells, *Solid State Electronics* 22 (1978) 193–197.
- [4] N.H. Reich, W.G.J.H.M. Van Sark, E.A. Alsema, R.W. Lof, R.E.I. Schropp, W.C. Sinke, W.C. Turkenburg, Crystalline silicon cell performance at low light intensities, *Solar Energy Materials and Solar Cells* 93 (2009) 1471–1481.
- [5] Michael D. Lammert, Richard J. Schwartz, The integrated back contact solar cell: A silicon solar cell for use in concentrated sunlight, *IEEE Transactions on Electron Devices* ED-24 (1997) 337–342.
- [6] R.A. Sinton, Young Kwark, J.Y. Gan, Richard M. Swanson, 27.5 Percent silicon concentrator solar cell, *IEEE Transactions on Electron Devices*, EDL-7 (1986) 567–569.
- [7] J. Coello, M. Castro, I. Anton, G. Sala, M.A. Vazquez, Conversion of commercial Si solar cells to keep their efficient performance at 15 Suns, *Progress in Photovoltaics: Research and Applications* 12 (2004) 323–331.
- [8] Swapan K. Datta, K. Mukhopadhyay, S. Bandopadhyay, H. Saha, An improved technique for the determination of solar cell parameters, *Solid State Electronics* 35 (1992) 1667–1673.
- [9] D.W. Cunningham, A. Parr, J. Posbic, B. Poulin, Performance comparison between BP solar mono and traditional multicrystalline modules, in: 23rd European PV Solar Energy Conference Proceedings, Sept. 2008.
- [10] B.C. Chakravarty, N.K. Arora, S.N. Singh, B.K. Das, Solar cell performance with an inhomogeneous grain size distribution, *IEEE Transactions on Electron Devices* ED-33 (1986) 158–160.
- [11] O. Breitenstein, J.P. Rakotoniaina, M.H. Al Rifai, M. Werner, Shunt type in crystalline silicon solar cells, *Progress in Photovoltaics: Research and Applications* 12 (2004) 529–538.
- [12] D.V. Lang, Deep-level transient spectroscopy: A new method to characterize traps in semiconductors, *Journal of Applied Physics* 45 (1974) 3023–3032.
- [13] S.N. Singh, Dinesh Kumar, Phenomenological model of anomalously high photovoltage generated in obliquely deposited semiconductor films, *Journal of Applied Physics* 103 (2008) 023713.1–023713.12.
- [14] A. Broniatowski, Measurement of the grain-boundary states in semiconductors by deep-level transient spectroscopy, *Physical Review B* 36 (1987) 5895–5905.
- [15] Priyanka Singh, S.N. Singh, M. Lal, M. Husain, Temperature dependence of  $I$ - $V$  characteristics and performance parameters of silicon solar cell, *Solar Energy Materials and Solar Cells* 92 (2008) 1611–1616.
- [16] J.D. Arora, A.V. Verma, Mala Bhatnagar, Variation of Series resistance with temperature and illumination level in diffused junction poly and single-crystalline silicon solar cells, *Journal of Materials Science Letters* 5 (1986) 1210–1212.
- [17] Daniel Macdonald, Andres Cuevas, Reduced fill factors in multicrystalline silicon solar cells due to injection-level dependent bulk recombination lifetimes, *Progress in Photovoltaics: Research and Applications* 8 (2000) 363–375.
- [18] H. Ohtsuka, M. Skameto, M. Loyama, K. Tsutsai, T. Uematsu, Y. Yazawa, Characteristics of bifacial solar cells under bifacial illumination with various intensity levels, *Progress in Photovoltaics: Research and Applications* 9 (2001) 1–13.